DOI: 10.1002/chem.200600726

Solid-State Self-Assembly of Polymeric Double Helicates Leading to Linear Arrays of Silver(I) Ions and Reversible Strand/Double Helix Interconversion in Solution

Adrian-Mihail Stadler,[a] Nathalie Kyritsakas,[b] Gavin Vaughan,[c] and Jean-Marie Lehn*[a]

Abstract: Reaction of a bent py-hyz-pym-hyz-pym **1** and of a linear py-hyz-py-hyz-pym **3** (py = pyridine; pym = pyrimidine; hyz = hydrazone) ligand strands with silver(I) tetrafluoroborate in CH_3NO_2 generates double-helical dinuclear **2** and trinuclear **4** complexes. These complexes form polymeric, highly ordered solid-state structures, with wirelike, linear continuous or discontinuous polycationic Ag_n^+ arrays with Ag−Ag distances of 2.78 to 4.42 Å. Ligand **5**, an isomer of **1**, is found to yield a [2×2] grid-type complex **6**. Titration experiments reveal the formation of linear rack-type dinuclear species from **1** and **5**. Acid–base modulated, reversible interconversion between strand **1** and double helicate **2** may be achieved by using tren as a competing complexing agent (tren = $N(CH_2CH_2NH_2)_3$). Progressive addition of silver(I) ions to a 1:1 mixture of **1** and **5** leads to the preferential formation of the double helicate **2** over the grid complex **6**, illustrating a process of self-organisation with selection of the correct ligand.

Keywords: coordination polymers · helical structures · hydrazones · self-assembly · silver · supramolecular chemistry

Introduction

The generation of double-helical metal complexes (helicates[1]) and their interconversion processes have attracted much attention in view of their analogy with important biological phenomena. The same holds for synthetic helical molecular strands[2a–c,3] and polymers.[2d] On the other hand, coordination polymers[4] and nanowire-type[5] electronic devices are one of the actual research targets in nanoscience, in view of their potential physical properties.

We report herein the formation of two double-helical complexes[6] by coordination of Ag^I ions to hydrazone-based ligand strands,[7,12] and their self-organisation in the solid state into polymetallic wirelike linear superstructures.

Helical strands containing hydrazone–pyrimidine (hyz-pym)[7] sequences were shown to have coordinative properties allowing the generation of sticklike and gridlike supramolecular complexes, on conversion of helicity codons into linearity codons upon complexation of appropriate metal ions (Pb^{II}, Zn^{II}) in an octahedral coordination geometry.[8] With several of these ligands, Ag^I was found to bind preferentially to the terminal hyz-py units (which contain the more basic pyridine nitrogen sites; Figure 1) in a distorted tetrahedral fashion, thus conserving the general helical

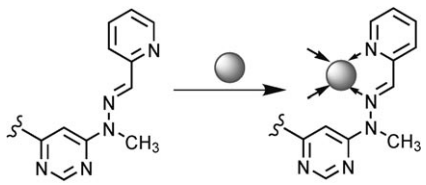

Figure 1. Silver(I) ion coordination to the hyz-py terminal units of the py-hyz-pym-hyz-py sequence of ligand strand **1**.

[a] Dr. A.-M. Stadler, Prof. Dr. J.-M. Lehn
Laboratoire de Chimie Supramoléculaire, ISIS
Université Louis Pasteur, 8 Allée Gaspard Monge
BP 70028, 67083 Strasbourg Cedex (France)
Fax: (+33) 390-245-140
E-mail: lehn@isis.u-strasbg.fr

[b] N. Kyritsakas
Service Commun de Rayons X, Institut Le Bel
Université Louis Pasteur, 4 Rue Blaise Pascal
67000 Strasbourg (France)

[c] Dr. G. Vaughan
European Synchrotron Radiation Facility (ESRF)
BP 220, 38043 Grenoble Cedex (France)

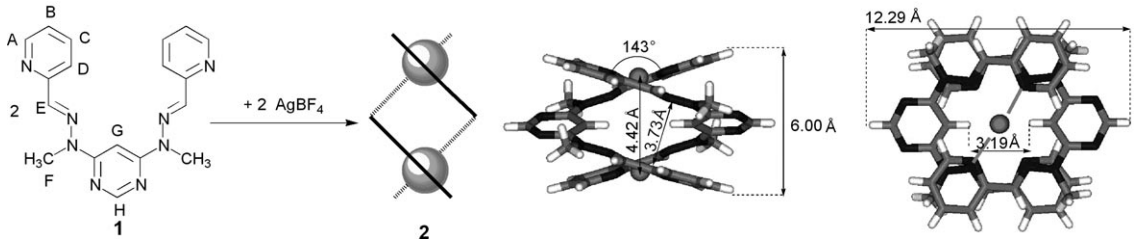

Figure 2. Formation and solid-state molecular structure of the double-helical complex **2** (BF_4^- ions are omitted for clarity) obtained by X-ray crystallography.

shape of the ligand and forming a double helix, as it has been observed in the case of pyridine–pyrimidine (py-pym) strands[9] (Figure 2).

Results and Discussion

Formation of the dinuclear double helicate 2 and its assembly into a linear polycationic $(Ag^I_2)_n$ array in the solid state: The treatment of the free ligand **1**,[7] containing two hydrazone groups, with one equivalent $AgBF_4$ in CH_3NO_2 leads to the dinuclear double-helical complex **2**, which was characterised by NMR spectroscopy (Figure 3) and X-ray crystallography (Figure 2).

The evolution of the system **1**/$AgBF_4$ was observed by ^{1}H NMR spectroscopy at 25 °C (400 MHz, Figure 3) when a solution of **1** in 2.5:1 $CD_3NO_2/CDCl_3$ was titrated with a solution of $AgBF_4$ in acetonitrile. By progressively adding portions of 0.1 equiv of $AgBF_4$ to **1** two steps can be identified. The first one, from 0 to 1 equiv of $AgBF_4$, shows the progressive consumption of ligand **1** and its conversion into a complex **2**, in a slow exchange system allowing the clear identification of the two species, the ligand and the complex. The second one, from 1.1 to 13 equiv of $AgBF_4$, shows the behaviour of the double-helical complex **2** in presence of an excess of $AgBF_4$, namely its stability in presence of an excess of metal salt and the slow exchange between it and the rack-type dinuclear compound (the peaks of which are indicated by triangles on the last top spectrum of Figure 3, bottom part), which may form with an excess of metal salt. Thus, a large excess of $AgBF_4$ (**1**/Ag^I = 1:12) produces a ≈85 % conversion of complex **2** into a new complex (proba-

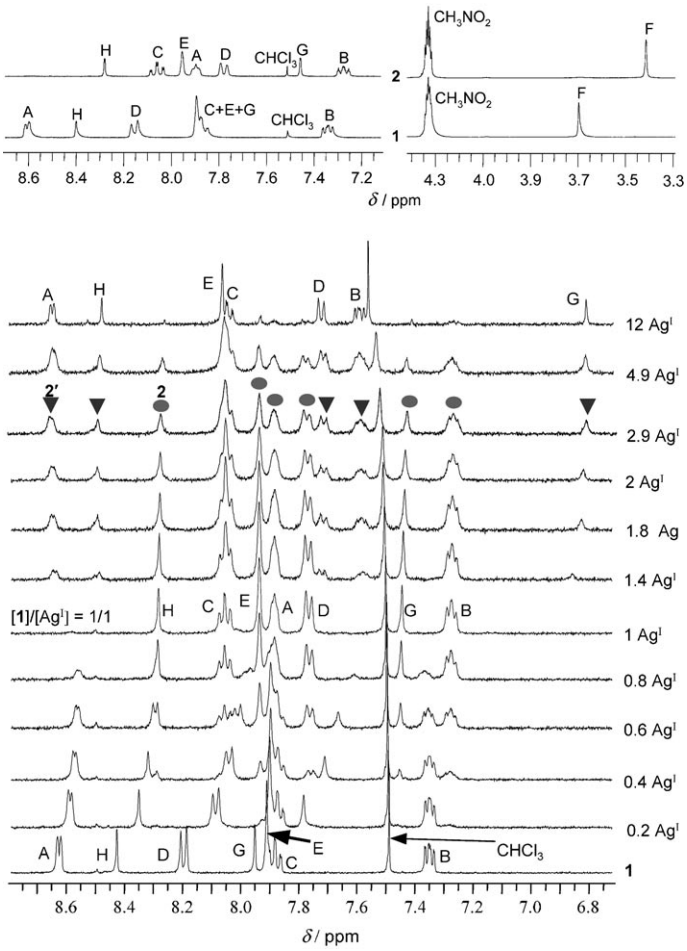

Figure 3. Top: 300 MHz ^{1}H NMR spectra of the ligand strand **1** and of its double helicate **2** formed by complexation of Ag^I ions ($AgBF_4$) in $CD_3NO_2/CDCl_3$ 4:1 at 25 °C. Bottom: NMR titration (^{1}H, 400 MHz) of ligand **1** with $AgBF_4$ in a $CD_3NO_2/CDCl_3$ 2.5:1 solvent mixture (only the aromatic parts of the spectra are shown).

Abstract in French: *La réaction d'un ligand coudé de type py-hyz-pym-hyz-pym **1** ou linéaire de type py-hyz-py-hyz-pym **3** (py = pyridine; pym = pyrimidine; hyz = hydrazone) avec $AgBF_4$ dans CH_3NO_2 engendre des complexes di-/tri-nucléaires de type double hélice. Ceux-ci forment à l'état solide des structures polymériques hautement ordonnées, présentant des "fils" polycationiques linéaires de type Ag_n^+, avec des distances Ag···Ag comprises entre 2.78 et 4.42 Å. Le ligand **5**, isomère du ligand **1**, donne naissance au complexe de type grille [2×2] **6**. Les titrages des ligands **1** et **5** par $AgBF_4$ ont mis en évidence la formation des complexes dinucléaires **2′** et **6′**. L'interconversion entre le ligand **1** et l'hélicate **2** peut être modulée par des ajouts alternatifs d'acide et de base, en utilisant le composé tren comme ligand compétitif. L'ajout progressif d'ions d'argent(I) à un mélange équimolaire des ligands **1** et **5** montre la formation préferentielle de l'hélicate **2** plutôt que de la grille **6**, illustrant ainsi un processus d'auto-organisation avec sélection du ligand approprié.*

bly with a linear racklike dinuclear structure **2′**; ≈15% of unconverted **2**). This behaviour may be compared with the one of the Pb^{II} gridlike complex formed by ligand **1**, which on adding of 1–1.5 equivalents of Pb^{II} led to fast conversion into the corresponding rack-type compound.[8] The species distribution graphs resulting from the analysis of the NMR spectra are shown in Figure 4. During the titration, progressive precipitation of the complex **2′** may occur.

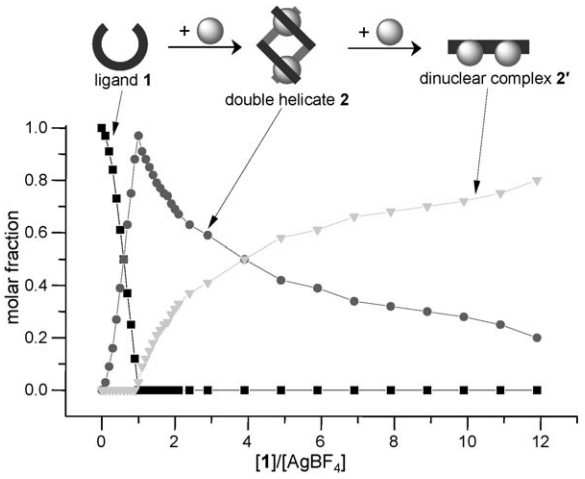

Figure 4. Distribution curves of the species formed on titration of a solution of ligand **1** in $CD_3NO_2/CDCl_3$ 2.5:1 by a solution of $AgBF_4$ in CD_3CN at 25°C. The data points were obtained from the integration of characteristic proton NMR signals.

The ^1H NMR data (Figure 3) showed that the complexation of the ligand with Ag^I ions and the formation of the double helix mainly produced a shielding effect ($\Delta\delta = \delta_{complex} - \delta_{ligand} < 0$) on the protons of the ligand molecule, due to the magnetic anisotropy of the pyrimidine and pyridine rings. The shielding decreased along the sequence: proton A ($\Delta\delta = -0.70$ ppm), proton G ($\Delta\delta = -0.44$ ppm), proton D (−0.37 ppm), proton F (−0.29 ppm), proton H (−0.12 ppm) and proton B (−0.06 ppm), with proton C (+0.19 ppm) and proton E (+0.06 ppm) being weakly deshielded. Such effects agree with the formation of a double-helical structure (see below). A ^1H-^{109}Ag HMQC (heteronuclear multiple quantum correlation) experiment showed a nuclear spin–spin coupling of the protons A, B, D and E with a silver ion ($\delta_{Ag} = 438.15$ ppm; reference $AgNO_3$; Figure 5).

Single crystals of complex **2** were obtained by diffusion of $(C_2H_5)_2O$ into a solution of the complex in CH_3NO_2. Radiocrystallographic analysis showed that the solid-state molecular structure of **2** ($[Ag_2(\mathbf{1})_2][BF_4]_2$) was a double helix with a C_2 symmetry axis passing through the Ag^I ions, leading to two identical moieties (Figure 2). Thus the unit is $Ag(\mathbf{1})BF_4$ and the crystal cell contains 8 such units. The two Ag^I ions of a complex present a distorted pseudotetrahedral coordination. The centroid-to-centroid internuclear distances between the pyridine nitrogen atoms and a silver ion are 2.17 and 2.19 Å, and the distances between the hydrazone nitrogen atoms and a silver ion are 2.64 and 2.70 Å. The N_{py}-Ag-N_{hyz} angles are 68.9 and 70.5°, when N_{py} and N_{hyz} are from the same strand and 114.3 and 113.6° when the two N atoms belong to different strands. The Ag–Ag internal distance is 4.42 Å (no internal contact between the silver (I) ions). The height of the cylinder defined by the helical strand in the complex is about 6 Å (centroid-to-centroid distance). The exterior diameter of the helix is 12.29 Å. The centroid-to-centroid distance between two opposed C5 pyrimidine protons is 3.19 Å (Figure 2), while the distances between the two pyridine nitrogen atoms coordinating the silver ion are 4.32 and 4.37 Å. The distance between the two ligand strands of about 3.7 Å suggests a weak π–π stacking interaction between the pyridine ring from one ligand and the hydrazone unit from the other.

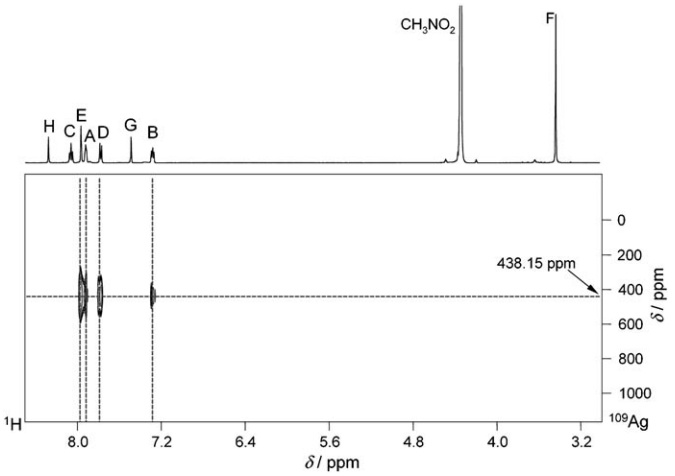

Figure 5. ^1H-^{109}Ag HMQC spectrum of complex **2** (CD_3NO_2, 500 MHz).

The electrospray mass spectrum (ES-MS) of complex **2** contains a peak corresponding to the species $[Ag_2(\mathbf{1})_2BF_4]^+$.

In the solid state, the double-helical complex **2** self-organises into a polymeric superstructure, with a Ag–Ag internuclear distance[10] of 3.02 Å (Figure 6, top), in agreement with related results.[9] The intercomplex stacking distance between two helical ligand branches is about 3.7 Å, comparable to the intracomplex one. No close contact between the terminal pyridines was observed, but a π–π stacking interaction between these rings (from a double-helical unit) and the hydrazone double bond (from a consecutive unit) may take place, the corresponding distance being about 3.7 Å (Figure 6, top). The centroid-to-centroid distance between the protons on C2 of two neighbouring polymeric entities is 4.36 Å.

In addition the crystal structure contains rows of BF_4^- counterions and cocrystallised CH_3NO_2 solvent molecules. The structural features indicate that complex **2** generates in the solid state a linear array of silver(I) ions, through intermolecular interactions between neighbouring complexes. DOSY (diffusion ordered spectroscopy) NMR experiments effected in CD_3NO_2 showed that in solution the complex is not present as a polymer, but as a monomeric double helix unit, yielding an average molecular diameter of 8.4 Å.

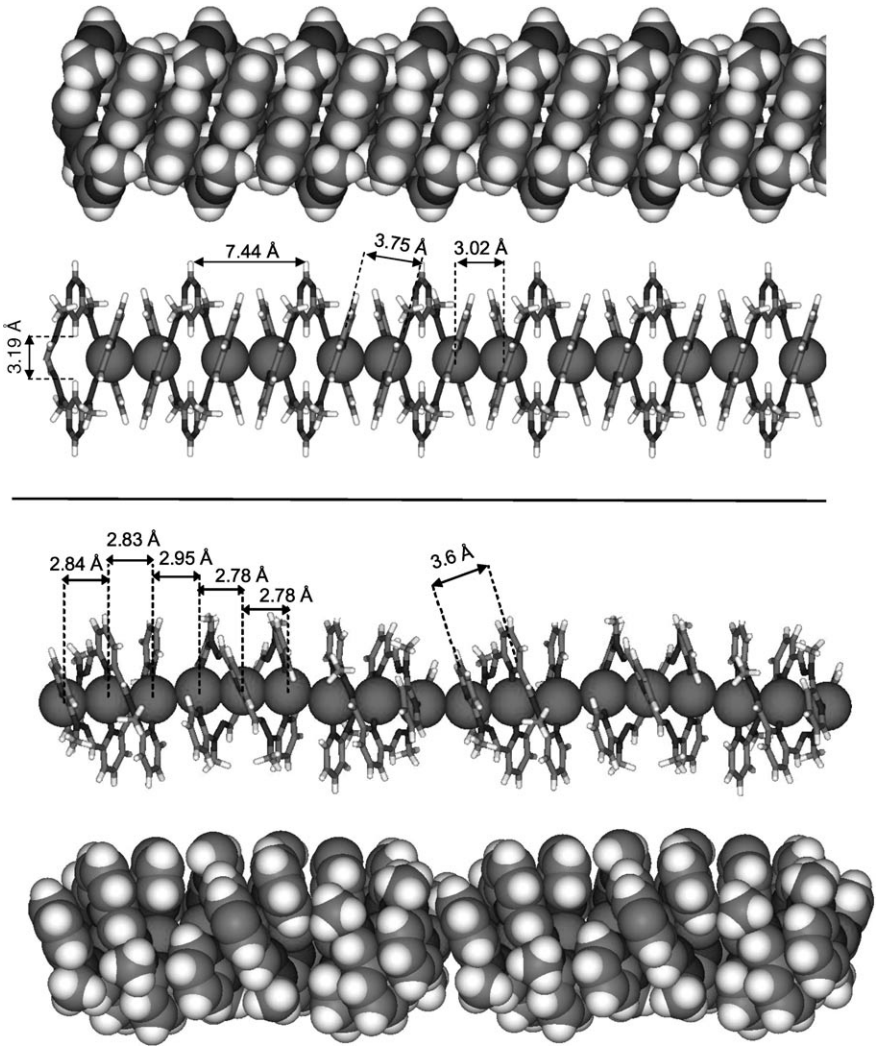

Figure 6. Solid-state polymeric superstructure formed by polyassociation of the double-helical complexes **2** (top) and **4** (bottom) from ligands **1** and **3**, respectively, showing the linear arrays of silver(I) ions obtained (BF_4^- ions are omitted for clarity).

A longer ligand of type **1** (containing four hydrazone bonds and having the central unit derived from 4,6-pyrimidine-dicarboxaldehyde)[7] forms a similar type of double-helical complex with Ag^I ions, as shown by ^1H-^1H NOESY experiments.

Strand 1/double-helicate 2 interconversion: Reversible interconversion between the free ligand **1** and the double-helical complex **2** may be induced by addition of a competing ligand through an acid–base neutralisation process[8,9] (Figure 7). Treating complex **2** with two equivalents of $N(CH_2CH_2NH_2)_3$ (tren) generates two $[Ag(tren)]^+$ complexes[11] and liberates ligand **1**. Adding to this mixture six equivalents of trifluoromethanesulfonic acid dissociates the $[Ag(tren)]^+$ complexes by protonation of the tren ligand and leads to the release of the Ag^I ions, which then bind to **1**, thus regenerating complex **2**. Subsequent deprotonation of $[trenH_3]^{3+}$ with six equivalents of Et_3N yields the ligand tren, which in turn abstracts the Ag^I ions from complex **2** to give back the free ligand **1**.

Formation of the trinuclear double helicate 4 and its assembly into a linear polycationic $(Ag^I_3)_n$ array in the solid state: Reaction of the pyridine–hydrazone (py-hyz-py-hyz-py) ligand **3** (prepared by condensation of 2,6-pyridine-dicarboxaldehyde with 2-(methylhydrazino)pyridine)[12] with an excess of $AgBF_4$ in nitromethane, leads to a complex that gives crystals of a trinuclear double-helical species (Figure 8) self-assembled into a solid-state polymeric polymetallic $(Ag^+_3\mathbf{3}_2)_n$ wire-like super-structure (Figure 6, bottom).

NMR titration of ligand **3** with $AgBF_4$, in $CD_3NO_2/CDCl_3$ 3:1 leads to the sequence of spectra showed in Figure 9. Adding from 0.1 to 1 equivalents of $AgBF_4$ produces dramatic and convergent changes in the spectrum. Then, adding from 1.1 to 1.5 equivalents of $AgBF_4$ produces a new sequence of convergent changes. Adding more than 1.5 equivalents of $AgBF_4$ gives only minor changes in the chemical shifts. This stoichiometry dependent evolution suggests that the formation of complex **4** (**3**/Ag^I = 1:1.5) passes through an intermediate mononuclear[12,15] complex (**3**/Ag^I = 1:1).

The ES-MS of a solution of ligand **3** with five equivalents of $AgBF_4$ in $CD_3NO_2/CDCl_3$ 3:1 contains a peak corresponding to the monocharged species: $[Ag_3(\mathbf{3})_2(BF_4)_2]^+$.

Single crystals of complex **4** were obtained by diffusion of iPr_2O into a solution of the complex in CH_3NO_2. The radiocrystallographic analysis showed that the unit cell of complex **4** contains 18 silver ions and 12 ligand units, that is, six trinuclear double helicates. Three consecutive double helicates are the repeating unit of the linear polynuclear polymer (Figure 10). Fixing the position of the first almost linear ($\approx$170°) N_{py}-Ag-N_{py} atom sequence of a double helix (this Ag^+ ion has the number 5 in the CIF file), the axis of the same sequence of the second and third double helices are turned by an average angle of about 60° (θ_1) and of about 115° ($\theta_1+\theta_2$) with respect to the first one (Figure 11). The corresponding angle for **2** is close to 0°.

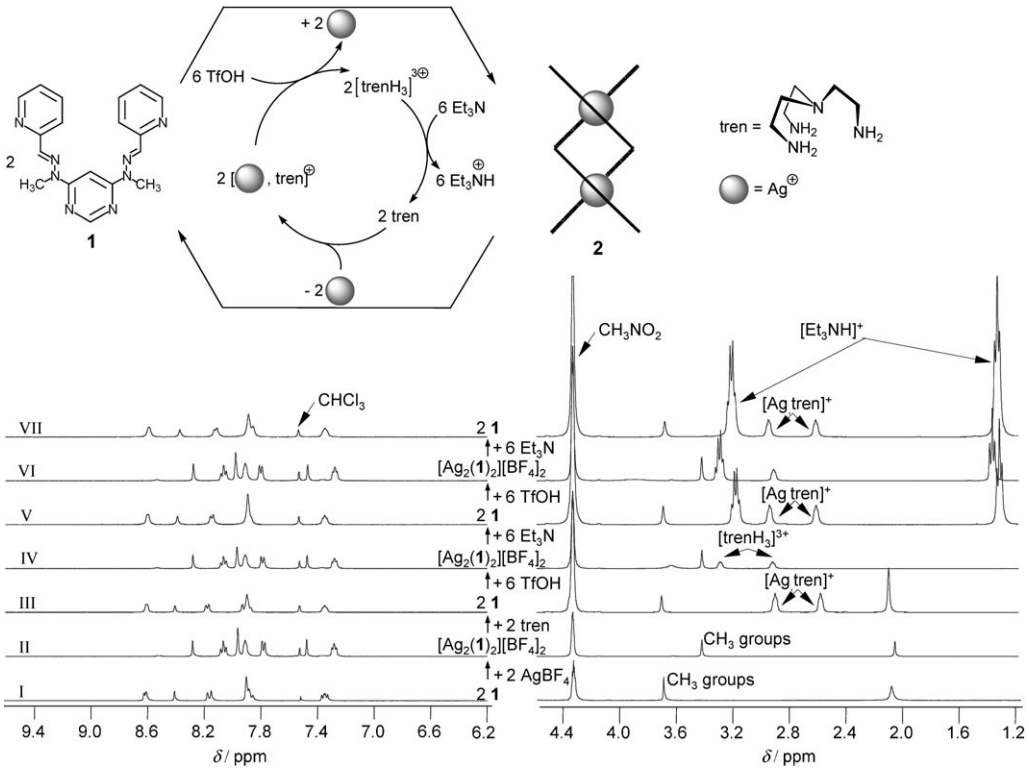

Figure 7. Top: Acid–base modulated reversible interconversion between the ligand strand **1** and its dinuclear double-helical silver(I) complex **2**. Bottom: ^{1}H NMR spectra corresponding to the process (400 MHz, $CD_3NO_2/CDCl_3$ 3:1).

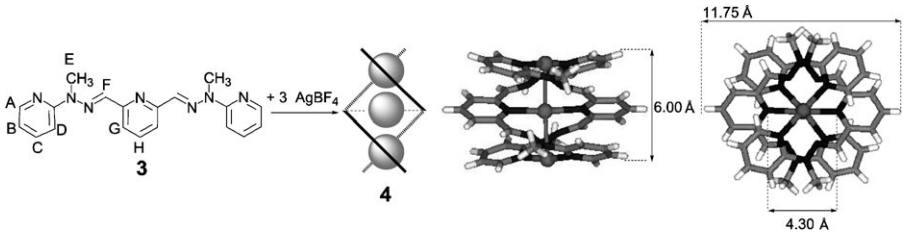

Figure 8. Formation from ligand **3** and X-ray crystallographic solid-state molecular structure of the trinuclear double-helical complex **4** (BF_4^- ions are omitted for clarity).

As in the case of the pyrimidine-based ligand **1** and its complex **2**, the two terminal pyridine units of each strand of the double helix **4** coordinate, two-by-two, to a silver ion (average N–Ag distance: 2.12 Å). The presence of a third pair of pyridine groups, with an intermediate position, allows the coordination of a third silver ion, inserted into the double helix between the two others (average N–Ag distance: 2.21 Å). The average N_{hyz}–Ag distance is 2.62 Å, while the average N_{py}–Ag distance is 2.16 Å, which suggests that the hydrazine sp^2 nitrogen atoms (N_{hyz}) coordinate less strongly than the pyridine ones (N_{py}).

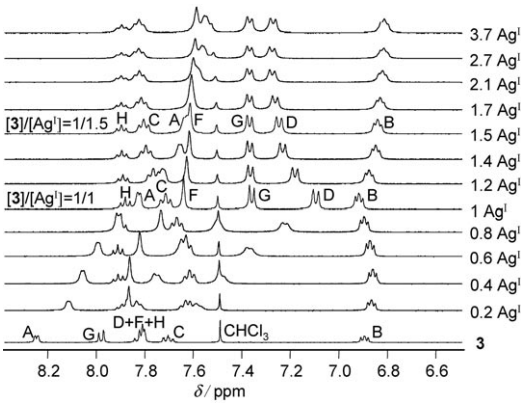

Figure 9. NMR titration (^{1}H, 400 MHz) of ligand **3** with $AgBF_4$ in a $CD_3NO_2/CDCl_3$ 3:1 solvent mixture (only the aromatic parts of the spectra are shown).

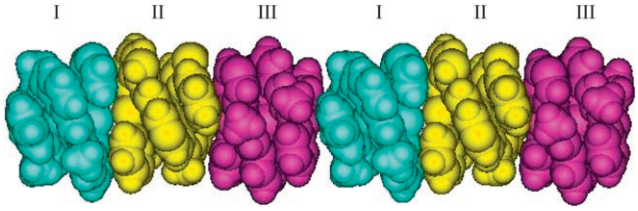

Figure 10. Representation of the linear solid-state polymer of **4** as a sequence of tris-double-helical, trinuclear basic motifs; I, II and III indicate first, second and third double helicate in a sequence.

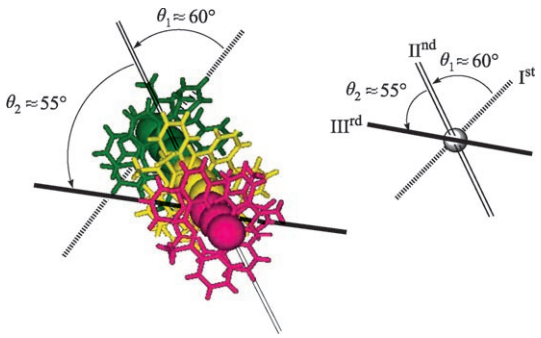

Figure 11. The motif generating the linear polymer of **4** consists of three double helices turned once with respect to the preceding one by about 55–60°.

The terminal silver ions have very distorted tetrahedral coordination geometry (almost a linear one with respect to the coordinating N_{py}), the main coordination function being accomplished by the N_{py} sites, while the N_{hyz} ones have a secondary role. The situation is similar for the central silver ion, which is mainly coordinated by the two N_{py} centres and is surrounded by four N_{hyz} "supporting" coordination site.

The average dihedral angles between two subsequent N_{py}-Ag-N_{py} sequences within a double-helical complex are of about 50° for complex **4** (ϕ_1 and ϕ_2), while for complex **2** the unique corresponding angle is of 67.2° (Figure 12).

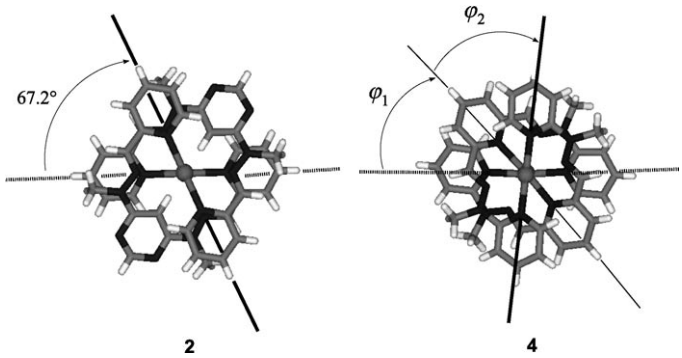

Figure 12. Angular parameters of the double-helical complexes **2** and **4**.

The Ag^+ ions define a one-dimensional $(Ag^+{}_3)_n$ polyionic "wirelike" structure with short Ag^+–Ag^+ distances (2.78, 2.83, 2.84 and 2.95 Å), the average distance being 2.86 Å. The Ag^+ sequence in **4** is continuous (Figure 6, bottom), whereas it is discontinuous for complex **2** (Ag^+–Ag^+ distance of 3.02 and 4.42 Å; Figure 2 and Figure 6, top). In both cases, the Ag^+–Ag^+ distances are of length similar to the interatomic distances in metallic silver (2.89 Å), but longer than the close ionic contact (the ionic radius of Ag^+ being of about 1.15 Å) and less than the van der Waals diameter (3.42 Å[13]). These data suggest a d^{10}–d^{10} homoatomic argentophilic[10,14] Ag^+–Ag^+ interaction.

The terminal pyridines of a double helix overlap partially with those of the following double helix, the average distance of about 3.7 Å suggesting the contribution of a π–π stacking interaction to the formation of the $\mathbf{4}_n$ polymer. Within a double helix, a similar distance is observed between the almost superimposed pyridine rings, corresponding to a π–π stacking interaction.

Formation of the [2×2] grid-type complex 6 from ligand 5: Ligand **5** may be considered as an isomeric strand of ligand **1** derived by positional rearrangement of the hydrazone group (Figure 13). Treatment of ligand **5** with one equivalent

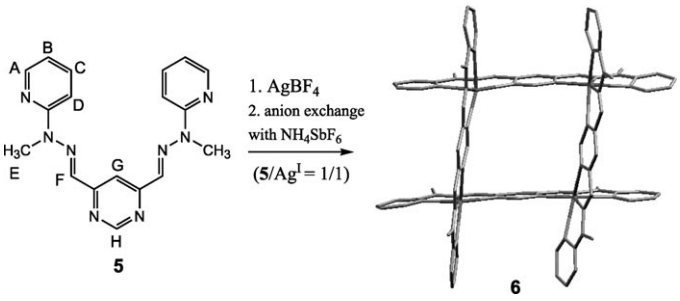

Figure 13. Ligand **5** and a low-quality X-ray molecular structure of its [2×2] gridlike complex **6** (SbF_6^- ions and solvent molecules are omitted for clarity).

of $AgBF_4$ in nitromethane led to dissolution of the ligand and allowed, after anion exchange with NH_4SbF_6, the crystallisation of a gridlike complex **6**. As the crystals were of low stability, it was impossible to obtain an X-ray structure of sufficient quality (for the obtained one the *R* factor is 16%), but the gridlike architecture is clearly shown (Figure 13). Moreover, the electrospray (ES) mass spectrum of a solution of **6** contains a peak at 2077.3000 which corresponds to the fragment $[Ag_4(\mathbf{5})_4(BF_4)_3]^+$ (calculated mass: 2077.2935).

^{1}H NMR spectroscopically observed titration of ligand **5** with $AgBF_4$ led to the sequence of spectra shown in Figure 14. Progressively adding amounts of 0.2 equiv of $AgBF_4$ to ligand **5** generates a continuous evolution of the spectra, with fast exchange on the NMR timescale, in line with the amount added, until a molar ratio $\mathbf{5}/Ag^I$ equal to 1:2, which corresponds to the formation of the dinuclear racklike complex **6′**; further addition of $AgBF_4$ produced no changes of the chemical shifts (Figure 14).

The chemical shifts of the signals of the spectrum corresponding to a $\mathbf{5}/Ag^I$ 1:1 molar ratio (the grid complex **6**) immediately changed on further addition of $AgBF_4$. Addition of one equivalent of $AgBF_4$ to the grid, converted it into the linear racklike dinuclear compound **6′**. This behaviour suggests that the grid **6** is more sensitive to the excess of $AgBF_4$ than the double helix **2**, given that an important excess of $AgBF_4$ is needed to convert the latter into the corresponding rack-type complex **2′**. Such a stoichiometry-dependent sensitivity of the grid **6** as compared to the double helicate **2** may be explained by the fact that in the grid **6** the octahedral coordination of Ag^I ions is less stable than the very dis-

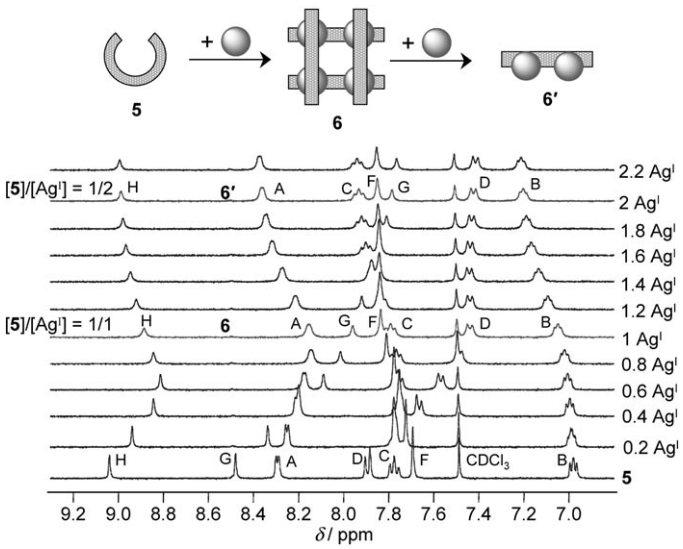

Figure 14. NMR titration (^{1}H, 400 MHz) of ligand **5** with $AgBF_4$ in a $CD_3NO_2/CDCl_3$ 3:1 solvent mixture (only the aromatic parts of the spectra are shown).

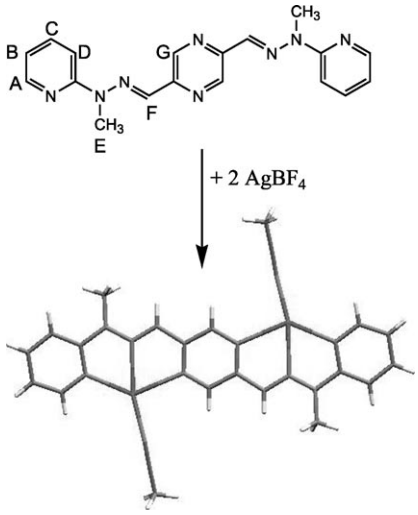

Figure 15. X-ray solid-state molecular structure of a dinuclear rack-type complex obtained from a pyrazine–bishydrazone ligand[17] by reaction with $AgBF_4$. BF_4^- ions are omitted for clarity. Ag^I ions are coordinated by the terpy-like tridentate sites and by a molecule of CH_3CN. Distances (Å): Ag–N_{py} 2.32, Ag–N_{hyz} 2.402, Ag–N_{pz} 2.469, Ag–N_{MeCN} 2.191. Angles (°): N_{pz}-Ag-N_{hyz} 67.9, N_{hyz}-Ag-N_{py} 67.1, N_{py}-Ag-N_{MeCN} 126.9, N_{MeCN}-Ag-N_{pz} 98.7.

torted tetrahedral, almost linear one found in the complex **2**.

Although we did not obtain crystals suitable for X-ray structure determination of the rack-type complexes **2′** (corresponding to ligand **1**) and **6′** (corresponding to ligand **5**), such structures were obtained for the corresponding Zn^{II} or Pb^{II} complexes of closely related ligands.[8,16] On the other hand such a solid-state molecular structure ($R \approx 6\%$) was obtained for a Ag^I dinuclear complex (Figure 15)[17] of a pyrazine-derived hydrazone-based ligand.[18] It shows indeed the dinuclear nature of the racklike complex, as well as the coordination of Ag^I ions by the terpy-like sites.

Self-selection in the self-assembly processes of ligands 1 and 5: The double helicate **2** and the grid complex **6** possess two degrees of isomerism: a first one due to the ligands **1** and **5** initial isomerism and a second one due to an identical 1:1 Ag^I/ligand molar ratio that leads to two different architectures. On the other hand, the isomerism of racklike dinuclear complexes **2′** (derived from ligand **1**) and **6′** (derived from ligand **5**) is solely due to the ligand.

Within the general framework of self-organisation with selection,[19,20] it is interesting to investigate the behaviour of a 1:1 mixture of the two isomeric ligands **1** and **5** in presence of $AgBF_4$. Titration of such a mixture with $AgBF_4$ in a $CD_3NO_2/CDCl_3$ 3:1 solvent was followed by ^{1}H NMR (400 MHz) at 25 °C (Figure 16).

The analysis of the spectra obtained leads to the following conclusions:

- At 1.5 equivalents of $AgBF_4$, the amount of ligand **1** is almost entirely converted into the double helicate **2**, while ligand **5** is in fast exchange with various complexes possibly up to complex **6** (Figure 16, spectrum IV). This clearly means that the complex **2** is more stable than both the grid **6** and an eventual mixed complex containing both ligands **1** and **5**. The preferential formation of the double helicate **2** implies the selection of only ligand molecules of type **1** and not of the isomeric ones, and thus involves self-selection[19,20] of the correct components of the dynamic mixture;

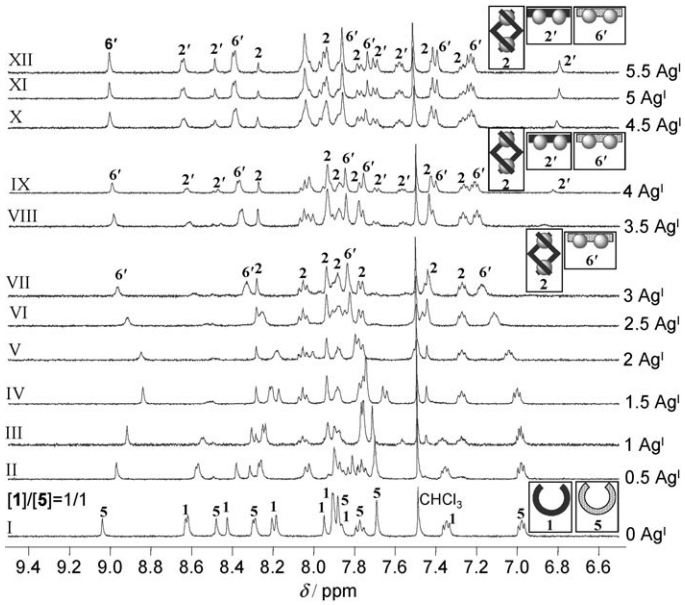

Figure 16. NMR titration (^{1}H, 400 MHz) of a 1:1 mixture of ligands **1** and **5** with $AgBF_4$ in a $CD_3NO_2/CDCl_3$ 3:1 solvent mixture at 25 °C (only the aromatic parts of the spectra are shown).

- At 2 equivalents of $AgBF_4$, the mixture is consists of both the double helicate **2** and the grid **6** (small changes in the proton chemical shifts with respect to the grid NMR spectrum in Figure 14 may be due to some fast exchanges or competitive equilibria). Further addition of $AgBF_4$ (less than 3 equiv) left the signals of **2** unchanged, but produced chemical shift changes in the spectrum of **6** (Figure 16, spectrum VI);
- At 3 equivalents of $AgBF_4$, ligand **5** exists almost solely as the dinuclear complex **6′** and ligand **1** mainly as double helicate **2** (Figure 16, spectrum VII);
- Further addition of $AgBF_4$ (up to 3.5 equiv) produces only minor changes in the spectrum of **6′** and, as expected (according to the titration from Figure 3, bottom), converts progressively the double helicate **2** into the dinuclear rack **2′** (Figure 16, spectra VIII-XII).

To summarise, addition of Ag^I ions to the 1:1 mixture of ligands **1** and **5** involves two selection processes within the constitutional dynamic mixture of equilibrating species: first, *component selection* of ligand **1** with respect to ligand **5** driven by the preferential formation of the double helicate **2** with respect to the grid **6**; second, the *self-selection* of ligand **1** over ligand **5** due to the preferred formation of the homostranded double helicate **2** with respect to a possible heterostranded one.

Conclusion

The present results show that the easily accessible hydrazone-connected ligands **1** and **3** react with Ag^I ions to produce the double-helical complexes **2** and **4** by coordination of the metal ions to the terminal py-hyz units of the two ligand strands. These complexes undergo polyassociation in the solid state to generate self-assembled highly ordered polymeric architectures containing linear arrays of silver ions, with, depending on the ligand structure, two types of polynuclear Ag^+ ionic sequences: a discontinuous one with ligand **1** and a continuous one with ligand **3**. Such architectures are models for linear wirelike polymetallic nanostructures and represent building blocks for the design of solid-state Ag^I-based metallosupramolecular assemblies.

The addition of silver(I) ions to the equimolar mixture of ligands **1** and **5** generates a dynamic mixture that reveals two selection processes: component selection and self-selection. Both features embody a process of self-organisation by selection.[20]

Experimental Section

Materials and general methods. The following reagents were prepared as previously described: **1**,[7] **3**[12] and **5**.[7] The following reagents were purchased from commercial sources: triethylamine (Lancaster, 99%), tren (Aldrich), triflic acid (Aldrich), $AgBF_4$ (Aldrich), CD_3CN (Eurisotop), CD_3NO_2 (Aldrich), $CDCl_3$ (Eurisotop; passed through basic alumina). Small traces of acid in nitromethane may induce minor changes in the chemical shift of ligands. To prevent this, it is useful to pass the nitromethane through basic alumina just before utilisation (preparation of the NMR tubes). $AgBF_4$ was kept under vacuum before use.

500 MHz ^{1}H spectra were recorded on a Bruker Ultrashield Avance 500 Spectrometer, 400 MHz ^{1}H spectra were recorded on a Bruker Ultrashield Avance 400 Spectrometer, 300 MHz ^{1}H spectra were recorded on a Bruker AM 300 spectrometer. The solvent signal was used as an internal reference for ^{1}H spectra (acetonitrile 1.94 ppm, nitromethane 4.33 ppm). For ^{109}Ag the reference was $AgNO_3$. The following notation is used for the ^{1}H NMR spectral splitting patterns: singlet (s), doublet (d), triplet (t), multiplet (m). 2D-NMR used experiments were: COSY (correlation spectroscopy), HMQC (heteronuclear multiple-quantum correlation (coherence)), NOESY (nuclear Overhauser enhancement spectroscopy or nuclear Overhauser and exchange spectroscopy), ROESY (rotating-frame Overhauser enhancement (effect) spectroscopy). Mass spectrometry measurements were performed by the Service de Spectrométrie de Masse, Université Louis Pasteur.

Synthesis of complex 2 ($[Ag_2(\mathbf{1})_2][BF_4]_2$): The complex was obtained by mixing ligand **1** (2 mg, 5.78 μmol, 1 equiv) with $AgBF_4$ (1.13 mg, 5.78 μmol, 1 equiv) in CD_3NO_2 (0.5 mL), which leads to complete dissolution of the ligand. ^{1}H NMR (CD_3NO_2/$CDCl_3$ 4:1, 300 MHz): $\delta = 8.28$ (d, $J = 0.9$ Hz, 2H; H_H), 8.06 (td, $J = 7.7$, 1.5 Hz, 4H; H_C), 7.95 (s, 4H; H_E), 7.92–7.87 (m, 4H; H_A), 7.78 (d, $J = 8.1$ Hz, 4H; H_D), 7.45 (d, $J = 0.9$ Hz, 2H; H_G), 7.31–7.24 (m, 4H; H_B), 3.41 ppm (s, 12H; H_F); ^{109}Ag NMR: $\delta = 438.15$ ppm; ES-MS: *m/z* calcd for $[Ag_2(\mathbf{1})_2BF_4]^+ = [C_{36}H_{36}N_{16}Ag_2BF_4]^+$: 995.144; found: 995.135.

Titration of ligand 1 with $AgBF_4$ and formation of complex 2′ ($[Ag_2(\mathbf{1})][BF_4]_2$): Ligand **1** (1.02 mg, 2.95 μmol, 1 equiv) was dissolved in $CDCl_3$ (200 μL) and introduced in a NMR tube, then CD_3NO_2 (500 μL; passed through basic alumina) was added. A solution of $AgBF_4$ (9.11 mg, 46.72 μmol, 15.84 equiv) in CD_3CN (320 μL) was prepared. The ligand solution was progressively titrated with portions of the $AgBF_4$ solution. Addition of 14 equivalents of $AgBF_4$ lead to a mixture of complexes **2** and **2′** that contains complex **2′** as the major compound (≈80–90%); it was not isolated. Progressive precipitation of the complex **2′** may occur. ^{1}H NMR (300 MHz): $\delta = 8.67$–8.63 (m, 2H, H_A), 8.49 (s, 1H, H_H), 8.06 (s, 2H, H_E), 8.05 (td, $J = 1.7$, 7.8 Hz, 2H, H_C), 7.70 (d, $J = 7.9$ Hz, 2H; H_D, 7.59 (ddd, $J = 1.3$, 5.0, 7.9 Hz, 2H; H_B), 6.77 (s, 1H; H_G), 3.71 ppm (s, 6H; H_F); ES-MS: *m/z* calcd for $[Ag_2(\mathbf{1})[BF_4]_2]^+ = [C_{18}H_{18}N_8Ag_2BF_4]^+$: 648.9782; found: 648.9941.

Synthesis of complex 4 ($[Ag_3(\mathbf{3})_2][BF_4]_2$): Complex **4** was obtained by mixing ligand **3** (2 mg, 5.78 μmol, 1 equiv) with $AgBF_4$ (1.7 mg, 4.34 μmol, 1.5 equiv) in CD_3NO_2/$CDCl_3$ 3:1 (0.5 mL). ^{1}H NMR (CD_3NO_2/$CDCl_3$ 3:1, 400 MHz): $\delta = 7.90$ (t, $J = 7.5$ Hz, 2H; H_H), 7.80 (t, $J = 7.9$ Hz, 4H; H_C), 7.68–7.58 (m, 8H; $H_A + H_F$), 7.37 (d, $J = 7.5$ Hz, 4H; H_G), 7.25 (d, $J = 8.3$ Hz, 4H; H_D), 6.84 (t, $J = 6.0$ Hz, 4H; H_B), 3.51 ppm (s, 12H; H_E); ES-MS (for a solution with **3**/$AgBF_4$ = 1:5): *m/z* calcd for $[Ag_3(\mathbf{3})_2(BF_4)_2]^+ = [C_{38}H_{38}N_{14}Ag_3B_2F_8]^+$: 1187.0623; found: 1187.0609.

Complexes 6 ($[Ag_4(\mathbf{5})_4][BF_4]_4$) and 6′ ($[Ag_2(\mathbf{5})][BF_4]_2$): Ligand **5** (1.52 mg, 4.39 μmol, 1 equiv) was dissolved in $CDCl_3$ (200 μL) and introduced in a NMR tube, then CD_3NO_2 (500 μL; passed through basic alumina) was added. A solution of $AgBF_4$ (2.2 mg, 11.22 μmol, 2.57 equiv) in CD_3CN (103 μL) was prepared. The ligand solution was progressively titrated with portions of 4 μL (0.1 equiv of Ag^I) of the $AgBF_4$ solution. After addition of 1 equivalent of $AgBF_4$, complex **6** was obtained; it was not isolated. ^{1}H NMR (400 MHz): $\delta = 8.87$ (s, 4H; H_H), 8.19–8.12 (br m, 8H; H_A), 7.96 (s, 4H; H_G), 7.84 (s, 8H; H_F), 7.79 (t, $J = 7.4$ Hz, 8H; H_C), 7.44 (d, $J = 9.4$ Hz, 8H; H_D), 7.08–7.01 (br m, 8H; H_B), 3.68 ppm (s, 24H; H_E); ES-MS: *m/z* calcd for $[Ag_4(\mathbf{5})_4(BF_4)_3]^+ = [C_{72}H_{72}N_{32}Ag_4B_3F_{12}]^+$: 2077.293; found 2077.3000.

Further addition of the rest of the $AgBF_4$ solution lead to complex **6′**, which was not isolated. ^{1}H NMR (300 MHz): $\delta = 9.00$ (d, $J = 1.1$ Hz, 1H; H_H), 8.40–8.36 (m, 2H; H_A), 7.94 (ddd, $J = 2.1$, 7.4, 8.7 Hz, 2H; H_C), 7.86 (s, 2H; H_F), 7.77 (d, $J = 1.1$ Hz, 1H; H_G), 7.42 (d, $J = 8.7$ Hz, 2H; H_D), 7.21 (ddd, $J = 0.8$, 5.0, 7.2 Hz, 2H; H_B), 3.72 ppm (s, 6H; H_E); ES-MS: *m/z* calcd for $[Ag_2(\mathbf{5})[BF_4]_2]^+ = [C_{18}H_{18}N_8Ag_2BF_4]^+$: 648.9782; found: 648.9821.

Crystals of **6** suitable for crystallographic determinations were obtained by diffusion of iPr$_2$O into a solution of **6** in CH_3NO_2 (very low quality crystals, however, allowing the observation of the Ag_4 square of the grid) or by adding an excess of NH_4SbF_6 to a solution of **6** in CH_3NO_2 (stirred overnight), followed by diffusion of iPr$_2$O into this solution (structure shown in Figure 13).

Acid–base neutralisation modulated 1⇌2 conversion (^{1}H NMR spectroscopy, 400 MHz; Figure 7): Ligand **1** (1.19 mg, 3.44 μmol, 1 equiv) was dissolved in $CDCl_3$ (150 μL) and introduced in a NMR tube (spectrum I), then CD_3NO_2 (450 μL; no special drying on basic alumina) was added. 50 μL of a solution of $AgBF_4$ (1.24 mg, 6.36 μmol, 1.85 equiv) in CD_3CN (93 μL) was added to the NMR tube solution, producing the conversion **1**→**2** (spectrum II). Tren (0.54 μL, 3.44 μmol, 1 equiv) was added to the NMR tube solution with a syringe, producing the conversion **2**→**1** (spectrum III). TfOH (0.91 μL, 10.32 μmol, 3 equiv) was added to the NMR tube solution with a syringe, producing the conversion **1**→**2** (spectrum IV). Et_3N (1.43 μL, 10.32 μmol, 3 equiv) was added to the NMR tube with a syringe, producing the conversion **2**→**1** (spectrum V). TfOH (0.91 μL, 10.32 μmol, 3 equiv) was added to the NMR tube solution with a syringe, producing the conversion **1**→**2** (spectrum VI). Et_3N (1.43 μL, 10.32 μmol, 3 equiv) was added to the NMR tube with a syringe, producing the conversion **2**→**1** (spectrum VII).

Titration of a 1:1 mixture of ligands 1 and 5 with $AgBF_4$ (observed by ^{1}H NMR spectroscopy, 400 MHz; see Figure 16): Ligands **1** (0.9 mg, 2.60 μmol, 1 equiv) and **5** (0.9 mg, 2.60 μmol, 1 equiv) were dissolved in $CDCl_3$ (150 μL), then CD_3NO_2 (450 μL) was added. A solution of ($AgBF_4$) (3.9 mg, 20 μmol, 7.7 equiv) in CD_3CN (154 μL) was prepared. The ligand mixture solution was progressively titrated with portions of 10 μL (0.5 equiv of Ag^I) of the $AgBF_4$ solution.

Crystal structure determinations: The crystals were obtained by diffusion–recrystallisation, by using the appropriate solvent/nonsolvent system: CH_3NO_2/Et_2O (**2**) or CH_3NO_2/iPr$_2$O (**4**).

X-ray-diffraction data for compound **2** were collected at the Service Commun de Rayons X, Université Louis Pasteur, Strasbourg. The crystals were placed in oil, and a single crystal was selected, mounted on a glass fibber and placed in a low-temperature N_2 stream (T=173 K). The X-ray-diffraction data were collected on a Nonius-Kappa-CCD diffractometer with graphite monochromatised $Mo_{K\alpha}$ radiation (λ=0.71073 Å), ϕ scans, by means of a "ϕ scan" type scan mode.

X-ray diffraction data measurements for compound **4** were carried out at the European Synchrotron Facility (beamline ID11) at Grenoble. A wavelength of 0.38745 Å was selected by using a double crystal Si(111) monochromator, and data were collected using a Bruker "Smart" CDD camera system at fixed 2θ. Data were reduced by using the Bruker SAINT software.

The structures were solved by direct methods and refined (based on F^2 with all independent data) by full-matrix least-squares methods (SHELXTL 97).

Crystallographic data for 2: $C_{20}H_{24}AgBF_4N_{10}O_4$ = 0.5 (2 $C_{18}H_{18}N_8Ag$·2 BF_4)·2 CH_3NO_2 = 0.5 (Ag_2(**1**)$_2$·2 BF_4)·2 CH_3NO_2; M_r = 663.17 g mol^{-1}; crystal system: monoclinic; space group: $C2/c$; a = 28.0983(3), b = 7.43520(10), c = 25.2142(3) Å; β = 94.923(5)°; V = 5248.23(12) Å^3; Z = 8; colour: yellow; crystal dimensions: 0.10×0.15×0.20 mm^3; ρ_{calcd} = 1.679 g cm^{-3}; F(000): 2672; μ = 0.845 mm^{-1}; transmission min/max: 0.9647/1.0000; T = 173(2) K; wavelength: 0.71073 Å; radiation: $Mo_{K\alpha}$ graphite monochromated; hkl limits: 0,39/0,10/−35,35; 2.83 ≤ θ ≤ 30.04°; number of data measured: 7626; number of data with $I > 2\sigma(I)$: 6721; number of variables: 366; R = 0.0314; R_w = 0.0819; GOF = 1.023; largest peak in final difference map: 0.464 e Å^{-3}.

Crystallographic data for 4: $C_{240}H_{272}Ag_{18}B_{18}F_{72}N_{96}O_{28}$ = 2[($C_{19}H_{19}N_7$)$_6$$Ag_9$]·12 CH_3NO_2·18 BF_4·4 H_2O = 2[(Ag_3(**3**)$_2$)$_3$]·12 CH_3NO_2·18 BF_4·4 H_2O; M_r = 8453.78 g mol^{-1}; crystal system: orthorhombic; space group: $Pbcn$; a = 25.532(2), b = 24.674(3), c = 23.312(4) Å; V = 14686(3) Å^3; Z = 2; colour: yellow; crystal dimensions: 0.30×0.30×0.35 mm^3; ρ_{calcd} = 1.912 g cm^{-3}; F(000): 8384; μ = 0.692 mm^{-1}; transmission min/max: 0.8192/0.7936; T: 393(2) K; wavelength: 0.38745 Å; radiation: synchrotron; hkl limits: −31,30/−30,29/−28,26; 1.02 ≤ θ ≤ 13.67; number of data measured: 70531; number of data with $I > 2\sigma(I)$: 11457; number of variables: 1007; R = 0.0691; R_w = 0.2006; GOF = 1.025; largest peak in final difference map: 2.023 e Å^{-3}.

CCDC-608238 (**2**) and CCDC-608239 (**4**) contain the supplementary crystallographic data for this paper. These data can be obtained free of charge from The Cambridge Crystallographic Data Centre via www.ccdc.cam.ac.uk/data_request/cif.

Acknowledgements

A.-M. S. thanks the Ministère de la Jeunesse, de la Recherche et des Nouvelles Technologies for a doctoral fellowship. We thank the European project AMNA for the financial support of a part of this work. We thank Prof. Pekka Pykkö for data on Ag–Ag interactions, Dr. Lionel Allouche for recording of DOSY, Dr. Roland Graff for recording of ^{1}H-^{109}Ag HMQC and Patrick Wehrung and Nathalie Zorn for mass spectra.

[1] a) J.-M. Lehn, A. Rigault, J. Siegel, J. Harrowfield, B. Chevrier, D. Moras, *Proc. Natl. Acad. Sci. USA* **1987**, *84*, 2565; b) J.-M. Lehn, *Supramolecular Chemistry—Concepts and Perspectives*, VCH, Weinheim, **1995**, Chapter 9; c) for an extensive review, see: C. Piguet, G. Bernardinelli, G. Hopfgartner, *Chem. Rev.* **1997**, *97*, 2005.

[2] For extensive reviews, see: a) S. H. Gellman, *Acc. Chem. Res.* **1998**, *31*, 173; b) A. E. Rowan, R. J. M. Nolte, *Angew. Chem.* **1998**, *110*, 65; *Angew. Chem. Int. Ed.* **1998**, *37*, 63; c) D. J. Hill, M. J Mio, R. B. Prince, T. S. Hughes, J. S. Moore, *Chem. Rev.* **2001**, *101*, 3893; d) B. Gong, *Chem. Eur. J.* **2001**, *7*, 4336; e) T. Nakano, Y. Okamoto, *Chem. Rev.* **2001**, *101*, 4013.

[3] a) V. Berl, I. Huc, R. G. Khoury, M. J. Krische, J.-M. Lehn, *Nature* **2000**, *407*, 720; b) V. Berl, I. Huc, R. G. Khoury, J.-M. Lehn, *Chem. Eur. J.* **2001**, *7*, 2798; c) V. Berl, I. Huc, R. G. Khoury, J.-M. Lehn, *Chem. Eur. J.* **2001**, *7*, 2810.

[4] a) D. Braga, F. Grepioni, G. R. Desiraju, *Chem. Rev.* **1998**, *98*, 1375; b) P. J. Hagrman, D. Hagrman, J. Zubieta, *Angew. Chem.* **1999**, *11*, 2798; *Angew. Chem. Int. Ed.* **1999**, *38*, 2638; c) M. Hong, W. Su, R. Cao, M. Fujita, J. Lu, *Chem. Eur. J.* **2000**, *6*, 427; d) S. R. Batten, *Curr. Opin. Solid State Mater. Sci.* **2001**, *5*, 107; e) C. Janiak, *Dalton Trans.* **2003**, 2781; f) G. S. Papaefstathiou, L. R. MacGillivray, *Coord. Chem. Rev.* **2003**, *246*, 169; g) S. Kitagawa, R. Kitaura, S. Noro, *Angew. Chem. Int. Ed.* **2004**, *43*, 2334; h) S. S. Y. Chui, M. F. Y. Ng, C.-M. Che, *Chem. Eur. J.* **2005**, *11*, 1739; i) for antimicrobial polymers, see: I. Francolini, V. Ruggeri, A. Martinelli, L. D'Ilario, A. Piozzi, *Macromol. Rapid Commun.* **2006**, *27*, 233; j) M. Rajeswaran, T. N. Blanton, D. J. Giesen, D. R. Withcomb, N. Zumbuliadis, B. J. Antalek, M. M. Neumann, S. T. Misture, *J. Solid State Chem.* **2006**, *179*, 1053; k) M. P. Suh, H. R. Moon, E. Y. Lee, S. Y. Jang, *J. Am. Chem. Soc.* **2006**, *128*, 4710; l) K. Matsumoto, Y. Harada, N. Yamada, H. Kurata, T. Kawase, M. Oda, *Cryst. Growth Des.* **2006**, *6*, 1083; m) J. R. A. Cottam, P. J. Steel, *J. Organomet. Chem.* **2006**, *691*, 2286.

[5] For ultrathin single-crystalline silver nanowire arrays formed in ambient solution phase, see: B. H. Hong, S. C. Bae, C.-W. Lee, S. Jeong, K. S. Kim, *Science* **2001**, *294*, 348.

[6] a) For a related silver complex, see: E. C. Constable, M. S. Khan, M. C. Liptrot, J. Lewis, P. R. Raithby, *Inorg. Chim. Acta* **1991**, *179*, 239; b) for a related bis-Na^I complex, see: T. W. Bell, H. Jousselin, *Nature* **1994**, *367*, 441.

[7] J.-L. Schmitt, A.-M. Stadler, N. Kyritsakas, J.-M. Lehn, *Helv. Chim. Acta* **2003**, *86*, 1598.

[8] A.-M. Stadler, N. Kyritsakas, R. Graff, J.-M. Lehn, *Chem. Eur. J.* **2006**, *12*, 4503.

[9] M. Barboiu, G. Vaughan, N. Kyritsakas, J.-M. Lehn, *Chem. Eur. J.* **2003**, *9*), 763.

[10] For extensive reviews see: a) M. Jansen, *Angew. Chem.* **1987**, *99*, 1136; *Angew. Chem. Int. Ed. Engl.* **1987**, *26*, 1098; b) P. Pykkö, *Chem. Rev.* **1997**, *97*, 597.

[11] a) S. G. Zipp, A. P. Zipp, S. K. Madan, *Coord. Chem. Rev.* **1974**, *14*, 29; for solid-state structures of silver(I) complexes with tris(2-aminoethyl)amines, see: b) E. C. Plappert, D. M. P. Mingos, S. E. Lawrence, D. J. Williams, *J. Chem. Soc. Dalton Trans.* **1997**, 2119; c) H. Zhang, J. Cai, X.-L. Feng, J.-Z. Liu, X.-Y. Li, L.-N. Ji, *Inorg. Chem. Commun.* **2001**, *4*, 241.

[12] M. A. Baldo, G. Chessa, G. Marangoni, B. Pitteri, *Synthesis* **1987**, 720–723.

[13] a) A. Bondi, *J. Phys. Chem.* **1964**, *68*, 441; b) R. Villanneau, A. Proust, F. Robert, P. Gouzerh, *Chem. Commun.* **1998**, 1491; c) G.-C. Guo, G.-D. Zhou, Q.-G. Wang, T. C. W. Mak, *Angew. Chem.* **1998**, *110*, 652; *Angew. Chem. Int. Ed.* **1998**, *37*, 630; d) M.-L. Tong, X.-M. Chen, B.-H. Ye, L.-N. Ji, *Angew. Chem.* **1999**, *111*, 2376; *Angew. Chem. Int. Ed.* **1999**, *38*, 2237; e) W. Su, M. Hong, J. Weng, R. Cao, S. Lu, *Angew. Chem.* **2000**, *112*, 3033; *Angew. Chem. Int. Ed.* **2000**, *39*, 2911; f) S. Yamada, T. Ishida, T. Nogami, *Dalton Trans.* **2004**, 898.

[14] a) M. A. Omary, T. R. Webb, Z. Assefa, G. E. Shankle, H. H. Patterson, *Inorg. Chem.* **1998**, *37*, 1380; b) E. J. Fernández, J. M. López-de-Luzuriaga, M. Monge, M. A. Rodríguez, O. Crespo, M. C. Gimeno, A. Laguna, P. G. Jones, *Inorg. Chem.* **1998**, *37*, 6002; c) M. A. Rawashdeh-Omary, M. A. Omary, H. H. Patterson, *J. Am. Chem. Soc.* **2000**, *122*, 10371; d) C.-M. Che, M.-C. Tse, M. C. W. Chan, K.-K. Cheung, D. L. Phillips, K.-H. Leung, *J. Am. Chem. Soc.* **2000**, *122*, 2464; e) Q.-M. Wang, T. C. W. Mak, *J. Am. Chem. Soc.* **2001**, *123*, 7594; f) A. N. Khlobystov, A. J. Blake, N. R. Champness, D. A. Lemenowskii, A. G. Majouga, N. V. Zyk, M. Schröder, *Coord. Chem. Rev.* **2001**, *222*, 155; g) Q.-M. Wang, T. C. W. Mak, *Angew. Chem.* **2001**, *113*, 1164; *Angew. Chem. Int. Ed.* **2001**, *40*, 1130; h) L. Pan, E. B. Woodlock, X. Wang, K.-C. Lam, A. L. Rheingold, *Chem. Commun.* **2001**, *18*, 1762–1763; i) M. J. Hannon, C. L. Painting, E. A. Plummer, L. J. Childs, N. W. Alcock, *Chem. Eur. J.* **2002**, *8*, 2226–2238; j) E. Bosch, C. L. Barnes, *Inorg. Chem.* **2002**, *41*, 2543–2547; k) S.-L. Zheng, M.-L. Tong, X.-M. Chen, *Coord. Chem. Rev.* **2003**, *246*, 185; l) O.-S. Jung, Y. J. Kim, Y.-A. Lee, S. W. Kang, S. N. Choi, *Cryst. Growth Des.* **2004**, *4*, 23; m) A. A. Mohamed, L. M. Pérez, J. P. Fackler, *Inorg. Chim. Acta* **2005**, *358*, 1657; n) L. Dobrzańska, H. G. Raubenheimer, L. J. Barbour, *Chem. Commun.* **2005**, 5050; o) L. Valencia, R. Bastida, A. Macías, M. Vicente, P. Pérez-Lourido, *New J. Chem.* **2005**, *29*, 424–426; p) P. J. Chmielewski, *Angew. Chem.* **2005**, *117*, 6575; *Angew. Chem. Int. Ed.* **2005**, *44*, 6417; q) X.-D. Chen, M. Du, T. C. W. Mak, *Chem. Commun.* **2005**, 4417; r) J.-P. Zhang, Y.-B. Wang, X.-C. Huang, Y.-Y. Lin, X.-M. Chen, *Chem. Eur. J.* **2005**, *11*, 552; s) H. Abbas, A. L. Pickering, D.-L. Long, P. Kögerler, L. Cronin, *Chem. Eur. J.* **2005**, *11*, 1071; t) D. R. Withcomb, M. Rajeswaran, *Polyhedron* **2006**, *25*, 1747; u) X. Liu, G.-C. Guo, M.-L. Fu, X.-H. Liu, M.-S. Wang, J.-S. Huang, *Inorg. Chem.* **2006**, *45*, 3679; v) R. P. Feazell, C. E. Carson, K. K. Klausmeyer, *Inorg. Chem.* **2006**, *45*, 2635.

[15] a) J. D. Curry; M. A. Robinson, D. H. Busch, *Inorg. Chem.* **1967**, *6*, 1570; b) D. Wester, G. J. Palenik, *J. Chem. Soc. Chem. Commun.* **1975**, *3*, 74; c) D. Wester, G. J. Palenik, *Inorg. Chem.* **1976**, *15*, 755; d) G. Paolucci, G. Marangoni, *Inorg. Chim. Acta* **1977**, *24*, L5; e) B. Chiswell, D. S. Litster, *Inorg. Chim. Acta* **1978**, *29*, 25; f) G. Bandoli, D. A. Clemente, G. Marangoni, G. Paolucci, *J. Chem. Soc. Chem. Commun.* **1978**, *6*, 235; g) G. Paolucci, G. Marangoni, G. Bandoli, D. A. Clemente, *J. Chem. Soc. Dalton Trans.* **1980**, *3*, 459; h) E. C. Constable, J. M. Holmes, *Inorg. Chim. Acta* **1987**, *126*, 187; i) M. Sakamoto, N. Matsumoto, H. Okawa, Hisashi, *Bull. Chem. Soc. Jpn.* **1991**, *64*, 691; j) A.-M. Stadler, J.-M. Lehn, unpublished results.

[16] M. Barboiu, J.-M. Lehn, *Proc. Natl. Acad. Sci. USA* **2002**, *99*, 5201–5206.

[17] The complex was obtained by mixing the ligand (1.17 mg, 3.38 μmol, 1 equiv) with $AgBF_4$ (2.55 mg, 13.08 μmol, 3.9 equiv) in CD_3CN (0.4 mL), which lead to complete dissolution of the ligand and to precipitation of the most part of the complex. ^{1}H NMR (CD_3CN, 300 MHz), after filtration: $\delta = 8.84$ (s, 2H; H_G), 8.30 (ddd, $J = 0.9$, 1.7, 4.9 Hz, 2H; H_A), 7.90 (s, 2H; H_F), 7.84 (ddd, $J = 1.9$, 7.2, 8.7 Hz, 2H; H_C), 7.47 (d, $J = 8.7$ Hz, 2H; H_D), 7.07 (ddd, $J = 0.9$, 4.9, 7.2 Hz, 2H; H_B), 3.65 (s, 6H; H_E). Crystals suitable for crystallographic determinations were obtained by diffusion of Et_2O into a solution of the complex in CH_3CN. Crystallographic data: $C_{22}H_{24}Ag_2B_2F_8N_{10} = C_{18}H_{18}N_8Ag_2{\cdot}2\,CH_3CN{\cdot}2BF_4$; $M_r = 817.87\ g\,mol^{-1}$; crystal system: triclinic; space group: $P\bar{1}$; $a = 6.3880(7)$, $b = 10.3780(9)$, $c = 10.8700(11)$ Å; $\alpha = 95.048(7)$, $\beta = 93.212(5)$, $\gamma = 102.248(4)°$, $V = 699.42(12)$ Å^3; $Z = 1$; colour: red; crystal dimensions: $0.10 \times 0.10 \times 0.10$ mm^3; $\rho_{calcd} = 1.942\ g\,cm^{-3}$; $F(000)$: 402; $\mu = 1.488\ mm^{-1}$; transmission min/max: 0.7551/0.7551; T: 173(2) K; wavelength: 0.71073 Å; radiation: $Mo_{K\alpha}$; hkl limits: $-8,8/-14,14/-14,15$; $2.62 \le \theta \le 30.08$; number of data measured: 4074; number of data with $I > 2\sigma(I)$: 3235; number of variables: 195; $R = 0.0526$; $R_w = 0.1523$; GOF = 1.000; largest peak in final difference map: 1.451 e Å^{-3}. CCDC-608541 contains the supplementary crystallographic data for this paper. These data can be obtained free of charge from The Cambridge Crystallographic Data Centre via www.ccdc.cam.ac.uk/data_request/cif.

[18] A.-M. Stadler, F. Puntoriero, S. Campagna, N. Kyritsakas, R. Welter, J.-M. Lehn, *Chem. Eur. J.* **2005**, *11*, 3997–4009.

[19] a) R. Krämer, J.-M. Lehn, A. Marquis-Rigault, *Proc. Natl. Acad. Sci. USA* **1993**, *90*, 5394; b) J. R. Nitschke, J.-M. Lehn, *Proc. Natl. Acad. Sci. USA* **2003**, *100*, 11970.

[20] J.-M. Lehn, *Proc. Natl. Acad. Sci. USA* **2002**, *99*, 4763.

Received: May 24, 2006
Published online: September 29, 2006

